DOI: 10.63527/1607-8829-2021-2-18-30

V.A.Romaka, *doc. techn sciences, professor*[1],
Yu.V. Stadnyk, *cand. chem. of science*[2],
V. V. Romaka, *doc. techn sciences,*
cand. chem. of science, professor[3]
Demchenko P.Yu., *cand. chem. of science*[2]
L.P. Romaka, *cand. chem. of science*[2],
V.Z. Pashkevych , *cand. tehn. of science*[1]
A.M. Horyn, *cand. chem. of science*[2],
A.Ya. Horpeniuk, *cand. tehn. of science*[1]

[1]National University "Lvivska Politechnika", 12, S. Bandera Str., Lviv, 79013, Ukraine,
e-mail: vromaka@polynet.lviv.ua;
[2]Ivan Franko National University of Lviv, 6, Kyryla and Mefodiya Str., Lviv, 79005, Ukraine,
e-mail: lyubov.romaka@lnu.edu.ua
[3]Technische Universität Dresden, Bergstrasse 66, 01069 Dresden, Germany

INVESTIGATION OF PROPERTIES OF NEW THERMOELECTRIC MATERIAL $Lu_{1-x}Sc_xNiSb$

The crystalline and electronic structures, thermodynamic, kinetic, energy and magnetic properties of the thermoelectric material $Lu_{1-x}Sc_xNiSb$ at temperatures T = 80 – 400 K have been studied. Depending on the concentration of the alloying component in the solid solution $Lu_{1-x}Sc_xNiSb$, different mechanisms of Sc atoms entering the semiconductor matrix have been established, which leads to different rates of generation of structural defects of acceptor and donor nature. The ratio of the concentrations of existing defects of donor and acceptor nature determines the position of the Fermi level ε_F and the conduction mechanisms in $Lu_{1-x}Sc_xNiSb$. The investigated solid solution $Lu_{1-x}Sc_xNiSb$ is a promising thermoelectric material. Bibl. 18, Fig. 8.

Key words: electronic structure, electric resistivity, Seebeck coefficient.

Introduction

In [1 – 7], a study of a new class of semiconductor thermoelectric materials based on *RNiSb* compounds (*R – Y, Gd – Lu*), which have a high efficiency of converting thermal energy into electricity [8], was initiated. The study of *RNiSb* compounds showed that they crystallize in the structural type of *MgAgAs* ($F\bar{4}3m$) [9], and their crystal structure is defective: in the crystallographic positions of 4*a* *R* atoms and 4*c* *Ni* atoms there are vacancies. In turn, these vacancies form in the band gap ε_g of *p-RNiSb* semiconductors structural defects of acceptor nature and the corresponding acceptor levels (zones), which confirm the results of kinetic studies [10].

Thermoelectric materials based on *p-RNiSb* (*R – Er, Lu*) [4 – 6] were obtained by doping semiconductors with *Zr* or *Sc* atoms by substituting rare earth metal atoms in the crystallographic position

4a. This was accompanied by the generation of structural defects of donor or neutral nature, which allowed to optimize the values of the of Seebeck coefficient $\alpha(T,x)$, thermal conductivity $\kappa(T,x)$ and electric conductivity $\sigma(T,x)$ [8]. Thus, doping *p*-(*Er*,*Lu*)*NiSb* with *Zr* atoms ($4d^25s^2$) [4, 5] led to the following changes in crystal and electronic structures:

– substitution at position 4*a* of *Er* or *Lu* atoms for *Zr* atoms generates structural defects of donor nature, because *Zr* has a larger number of *d*-electrons than, for example, the *Lu* atom ($5d^16s^2$). In this case, an impurity donor zone ε_D^1 appears in the band gap ε_g;

– occupation of vacancies in position 4*a* by *Zr* atoms simultaneously eliminates structural defects of acceptor nature and generates defects of donor nature and donor zone ε_D^2.

In the case of doping of *p-ErNiSb* with *Sc* atoms ($3d^14s^2$) in the $Er_{1-x}Sc_xNiSb$ semiconductor, no donor level was formed, because *Er* and *Sc* atoms are located in the same group of the Periodic Table of the Elements [6]. On the other hand, the occupation of vacancies in position 4*a* by *Sc* atoms creates defects of donor nature with the appearance of the donor zone ε_D^2 in the band gap ε_g.

The following results of the study of structural, thermodynamic, kinetic, energy and magnetic properties of semiconductor solid solution $Lu_{1-x}Sc_xNiSb$ will establish the nature of structural and energy defects, which will make the process of optimizing the characteristics of thermoelectric material predictable to maximize thermal energy conversion efficiency.

Research methods

The crystal structure, the distribution of the density of electronic states (DOS), and the magnetic, thermodynamic, kinetic, and energy properties of $Lu_{1-x}Sc_xNiSb$ have been studied. The samples were synthesized by fusing the charge of the initial components in an electric arc furnace in an inert argon atmosphere, followed by homogenizing annealing for 720 h at a temperature of 1073 K. Diffraction data arrays were obtained using a powder diffractometer STOE STADI P ($Cu\text{K}\alpha_1$-radiation). Crystallographic parameters were calculated using the program Fullprof [11]. The chemical and phase compositions of the samples were monitored by an energy-dispersive *X*-ray analyzer (EPMA) [12]. Calculations of DOS, electron localization function (ELF), enthalpy of mixing (ΔH_{mix}), and optimization of $Lu_{1-x}Sc_xNiSb$ crystal structure parameters were performed using the Korringa-Kohn-Rostocker (KKR) method in the coherent potential (CPA) and local density approximation (LDA) and the full-potential method of linearized plane waves (FLAPW). KKR simulations were performed using the AkaiKKR software package [13] in the local density approximation for the exchange-correlation potential with parameterization by Moruzzi, Janak, Williams [14] in the semi-relativistic consideration of the core level and spin-orbit interaction. Elk software package was used in FLAPW calculations [15]. Calculations were performed for a 10×10×10 *k*-grid in both the LDA and generalized gradient approximations (GGA). The Brillouin zone was divided into 1000 *k*-points, which were used to calculate the Bloch spectral function (band spectrum) and the density of electronic states. The width of the energy window was chosen so as to capture the semi-core states of the *p*-elements. Visualization of volumetric data was performed using the program VESTA [16]. Topological analysis and interpretation of DOS and ELF was performed within the framework of Bader's theory [10]. The accuracy of calculating the position of the Fermi level was $\varepsilon_F \pm 6$ meV. Temperature and concentration dependences of resistivity (ρ) and the Seebeck coefficient (α) were measured with respect to copper and magnetic susceptibility (χ) (Faraday's method) of $Lu_{1-x}Sc_xNiSb$ samples, $x = 0 – 1.0$, in the temperature range $T = 80 – 400$ K.

Investigation of structural characteristics of $Lu_{1-x}Sc_xNiSb$

Microprobe analysis of the concentration of atoms on the surface of the samples established their correspondence to the initial composition of the charge (Fig. 1), and *X*-ray phase and structural analyzes showed that the diffraction patterns of samples $Lu_{1-x}Sc_xNiSb$, $x = 0 - 0.1$, and *ScNiSb* are indexed in the *MgAgAs* [9] structural type and contain no traces of other phases (Fig. 2*a*).

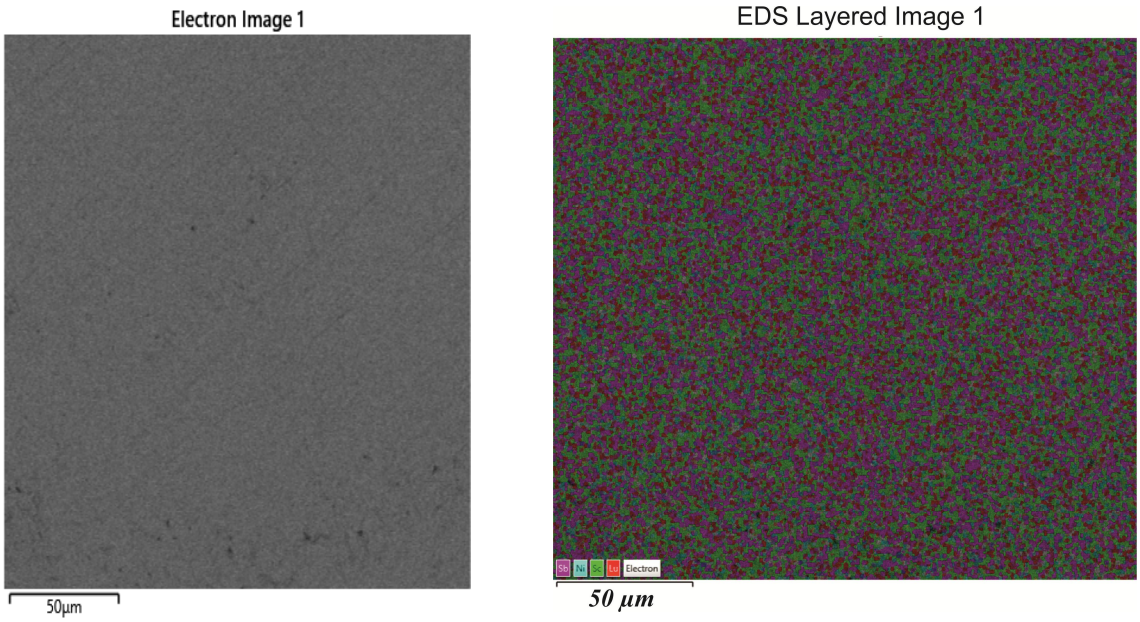

a) *b)*

Fig. 1. Photograph of the surface (a) and distribution of components (b) of the sample $Lu_{0.98}Sc_{0.02}NiSb$

Given that the atomic radius of *Lu* ($r_{Lu} = 0.173$ nm) is larger than *Sc* ($r_{Sc} = 0.164$ nm), it is assumed that the values of the unit cell period a(*x*) $Lu_{1-x}Sc_xNiSb$ decrease when the *Lu* atoms are replaced by *Sc* atoms (Fig. 4*a*. 2*b*). In this case, structural defects of neutral nature are generated in the $Lu_{1-x}Sc_xNiSb$ semiconductor (*Lu* and *Sc* atoms contain the same number of external *d*-electrons). However, as can be seen from the insert of Fig. 2*b*, the decrease in the values of the period a(*x*) $Lu_{1-x}Sc_xNiSb$ at concentrations *x*=0–0.1 is nonlinear, which may indicate more complex structural changes than the replacement of *Lu* atoms by *Sc*. Such changes can be caused by partial occupation of *Sc* vacancies at positions 4*a* of *Lu* atoms and/or 4*c Ni* atoms. This will lead to the deformation of the unit cell and change its period a(*x*). However, the accuracy of *X*-ray diffraction studies does not directly identify these changes.

Therefore, from the results of *X*-ray structural studies we can assume that the structure of the semiconductor $Lu_{1-x}Sc_xNiSb$ may simultaneously undergo the following changes:

– substitution at position 4*a* of *Lu* atoms by *Sc* atoms generates defects of neutral nature;

– occupation of vacancies in position 4*a* by *Sc* atoms simultaneously eliminates the structural defect of acceptor nature and the corresponding acceptor zone ε_A^1 in the band gap ε_g. At the same time, structural defects of donor nature and the corresponding donor zone ε_D^1 are formed;

– occupation of vacancies by *Sc* atoms in position 4*c* of *Ni* atoms simultaneously eliminates structural defects of acceptor nature and the corresponding acceptor zone ε_A^2, and in the band gap ε_g a structural defect of donor nature is formed with the appearance of donor zone ε_D^2.

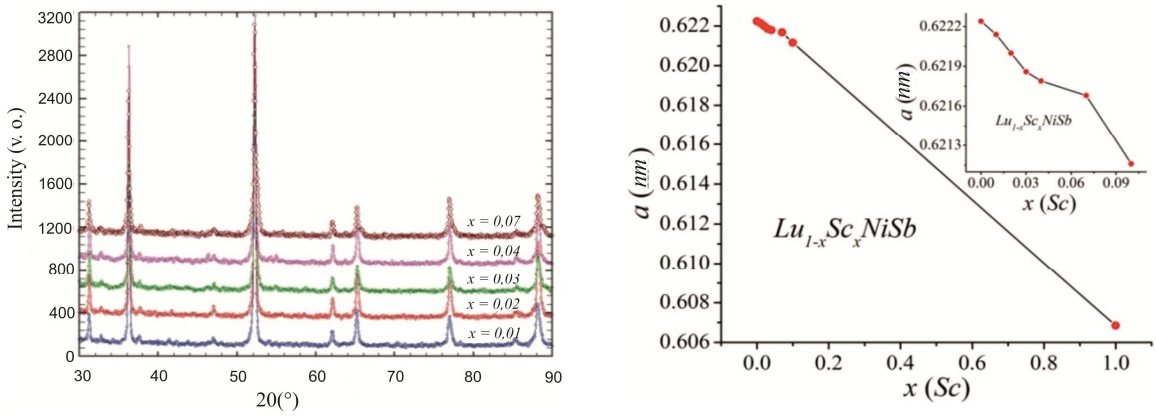

a) *b)*

Fig. 2. Diffractograms of samples (a) and change of the period of the unit cell a (x) (b) $Lu_{1-x}Sc_xNiSb$

We simulated the change in the values of the period of the unit cell a(x) $Lu_{1-x}Sc_xNiSb$ for the ordered variant of its crystal structure (all atoms occupy their own crystallographic positions) using software packages AkaiKKR [13] and Elk [15] (Fig. 3*a*).

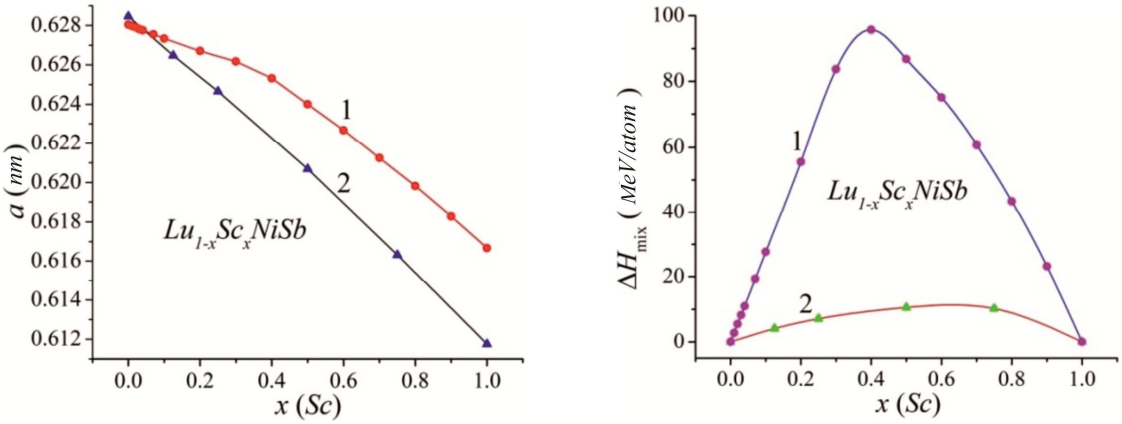

a) *b)*

Fig. 3. Calculation of the change in the period of the unit cell a(x) (a) and the enthalpy of mixing ΔH(x) (b) solid solution $Lu_{1-x}Sc_xNiSb$: 1 – software package AkaiKKR, 2 – software package Elk

The results of modeling a(x) $Lu_{1-x}Sc_xNiSb$ are close to the results of *X*-ray diffraction studies (Fig. 2*b*). Using the Elk software package we get a linear decrease of a(x) $Lu_{1-x}Sc_xNiSb$, whereas modeling with the AkaiKKR software package yields an inflection of $x \approx 0.4$ on the dependence of a(x).

Modeling of the electronic structure and experimental studies of the properties of $Lu_{1-x}Sc_xNiSb$ will show the degree of adequacy of the assumptions made and will allow us to understand the mechanism of entry of *Sc* atoms into the *p-LuNiSb* matrix.

Modeling of thermodynamic characteristics and electronic structure of $Lu_{1-x}Sc_xNiSb$

Modeling of thermodynamic characteristics for a hypothetical solid solution $Lu_{1-x}Zr_xNiSb$, $x = 0 – 1.0$, in the approximation of harmonic oscillations of atoms in the framework of density functional theory (DFT) allows us to establish the energy feasibility of the existence of a substitutional solid solution. Fig.3*b* shows the results of modeling by the KKR [13] and FLAPW [15] methods of changing the enthalpy of mixing $\Delta H_{mix}(x)$ $Lu_{1-x}Zr_xNiSb$. The nature of the behavior of the $\Delta H_{mix}(x)$ dependences obtained by both modeling methods shows the energy feasibility of the existence of a substitutional solid solution for the studied $Lu_{1-x}Zr_xNiSb$, $x = 0 – 0.10$. In turn, the dependences $\Delta H_{mix}(x)$ $Lu_{1-x}Zr_xNiSb$ differ slightly. Thus, the dependence $\Delta H_{mix}(x)$, obtained using the Elk software package [15], shows that its growth in the concentration range $x = 0 – 0.4$ is associated with the energy feasibility of forming a substitutional solid solution when *Lu* atoms in crystallographic position 4*a* are replaced of atoms *Sc*. In addition, from Fig. 3*b*, curve 1, it is also seen that the enthalpy dependence of the mixing $\Delta H_{mix}(x)$ $Lu_{1-x}Sc_xNiSb$ passes through the maximum at $x \approx 0.4$, and then decreases monotonically. In turn, the dependence $\Delta H_{mix}(x)$ $Lu_{1-x}Sc_xNiSb$, obtained using the software package AkaiKKR [13], contains a maximum of $x \approx 0.7$.

Important parameters that characterize the results of doping the *LuNiSb* semiconductor with *Sc* atoms to obtain the thermoelectric material $Lu_{1-x}Sc_xNiSb$ are the behavior of the Fermi level ε_F, the band gap ε_g and the zones of continuous energies. Based on the assumption that the crystal structure of $Lu_{1-x}Sc_xNiSb$ is ordered, using the Elk software package [15], the distribution of the density of electronic states (DOS) was modeled (Fig. 4*a*). It is seen that in *LuNiSb* the Fermi level ε_F lies in the middle of the band gap ε_g, which is characteristic of intrinsic semiconductors [17], and the band gap $\varepsilon_g = 190.5$ meV.

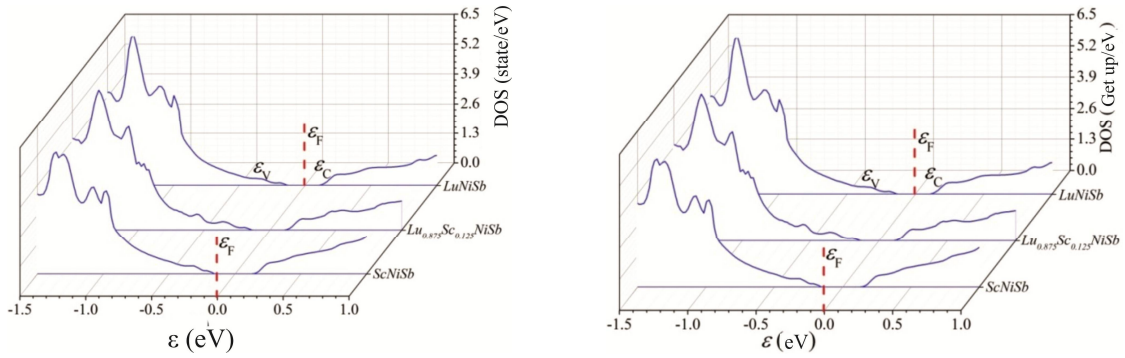

a) *b)*

Fig. 4. Calculation of DOS (Elk software package) for ordered (a) and unordered (AkaiKKR software package) (b) variants in the crystal structure $Lu_{1-x}Sc_xNiSb$

The results of DOS modeling for the ordered variant of the crystal structure $Lu_{1-x}Sc_xNiSb$, $x = 0.125$, (Elk software package [15]) show the redistribution of DOS (Fig. 4*a*) and the increase in the band gap ε_g. The Fermi level ε_F lies in the middle of the band gap ε_g, because the atoms *Lu* and *Sc* are located in the same group of the Periodic Table of the Elements, and the generated structural defects are neutral.

DOS simulation for the ordered variant of the *ScNiSb* crystal structure ($Lu_{1-x}Sc_xNiSb$ for $x = 1.0$) gives a band gap $\varepsilon_g = 247.6$ meV, which is greater than that of *LuNiSb*. In this case, the Fermi level ε_F also lies in the middle of the band gap ε_g. We can predict that *p-ScNiSb* will become the basic semiconductor for thermoelectric materials.

Therefore, DOS simulations for the ordered variant of the *LuNiSb* and *ScNiSb* structure do not correspond to the results of experiment [2, 3, 5, 6], which show that the main carriers are holes (*p*-type

conductivity) and the Fermi level ε_F lies near the valence band ε_V. Based on these results, a model of the crystal structure of *p-LuNiSb* and *p-ScNiSb* was proposed, the essence of which is the presence of vacancies in positions 4*a* and 4*c* of *Lu* (*Sc*) and *Ni* atoms, respectively.

The DOS calculation for the disordered variant of the $Lu_{1-x}Sc_xNiSb$ crystal structure (Fig. 4*b*) was performed using the model we proposed in the DOS calculations for the *YNiSb* compound [7]. The model of the structure of the semiconductor $Lu_{1-x+y}Sc_xNi_{1-2y}Sb$ is considered, in which at position 4*a* the *Lu* atoms are replaced by *Sc* atoms. In addition, the *Lu* atoms partially move to the 4*c* position of the *Ni* atoms, and a vacancy (Vac) occurs simultaneously in this position. Moreover, how many *Lu* atoms additionally move to the 4*c* position of *Ni* atoms, so many vacancies appear in this position. That is, if the atoms of *Lu* at the number x=0.01 move to the position 4*c* of the atoms of *Ni*, then there are additional vacancies with a concentration of x=0.01 Therefore, at position 4*c* of *Ni* atoms we have: Ni – $x = 0.98$, Lu – $x = 0.01$, Vac – $x = 0.01$. In this model of the $Lu_{1-x}Sc_xNiSb$ crystal structure, the calculation of the distribution of DOS shows the presence of the band gap ε_g, and the Fermi level ε_F lies near the valence band ε_V (Fig. 4*b*). This means that the values of the Seebeck coefficient $\alpha(T,x)$ at all investigated concentrations and temperatures will be positive in the experiment.

It is clear that this model is correct only for a small number of *Sc* impurity atoms, because even partial occupation of the position 4*c* of *Ni* atoms by *Lu* atoms significantly deforms the structure with its subsequent decay. The disadvantage of this model is also the generation of a significant number of energy levels in the band gap ε_g, which intersect with the zones of continuous energies and fix the Fermi level εF. This makes it difficult to determine the real band gap ε_g and the value of the activation energy $\varepsilon_1^{\rho}(x)$ from the Fermi level ε_F to the valence band ε_V.

Modeling the electron density distribution and the Elk electron localization function by introducing *Sc* atoms into the *LuNiSb* compound structure by substituting *Lu* atoms in the 4*a* crystallographic position (Fig. 5) gives a clear idea of changes in the crystal and electronic structures of $Lu_{1-x}Sc_xNiSb$ thermoelectric material.

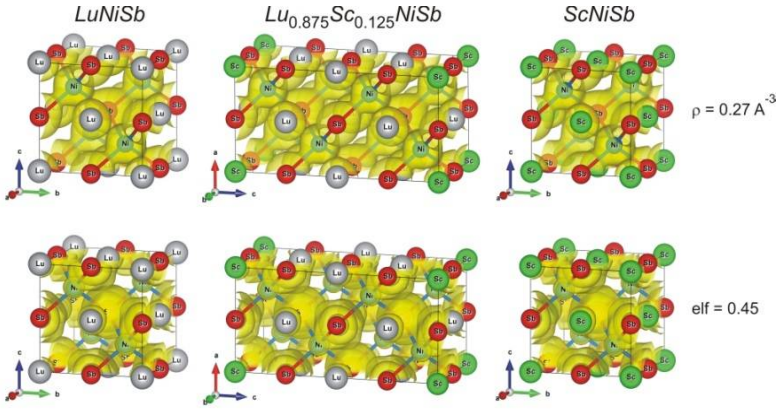

Fig. 5. Simulation of electronic density of $Lu_{1-x}Sc_xNiSb$, x=0–1.0, (Elk software package)

The following results of experimental studies of kinetic, energy and magnetic properties will show the degree of adequacy of the proposed disordered model of the crystal structure of $Lu_{1-x}Sc_xNiSb$ to the real structure of the semiconductor.

Investigation of kinetic, energy and magnetic properties of $Lu_{1-x}Sc_xNiSb$

Temperature and concentration dependences of resistivity ρ and the Seebeck coefficient α of Lu_{1-}

$_xSc_xNiSb$ samples are shown in Fig. 6, 7. The dependences ln(ρ(1/*T*)) and α(1/*T*) are typical for doped and compensated semiconductors with high- and low-temperature activation sites, which indicates the presence of several activation mechanisms of conductivity [17]. In addition, high-temperature activation regions on the ln(ρ(1/*T*)) dependences for all studied samples $Lu_{1-x}Sc_xNiSb$ (Fig. 6*a*) show that the Fermi level ε_F is located in the forbidden band ε_g, and positive values of the Seebeck coefficient α(*T*) (Fig. 6*b*) that specify its position – near the valence band ε_V. Thus, holes are the main carriers of $Lu_{1-x}Sc_xNiSb$ electricity at almost all temperatures studied.

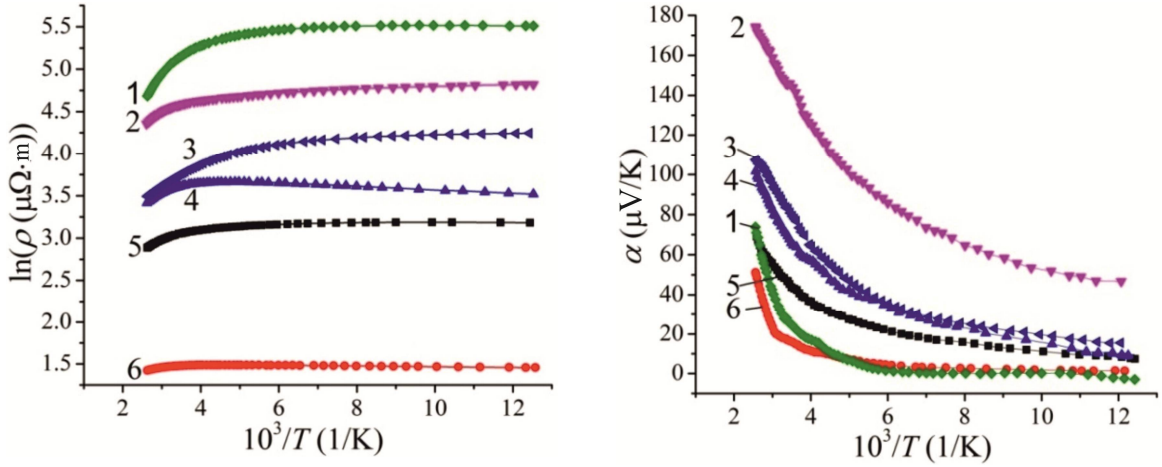

a) *b)*

Fig. 6. Temperature dependences of resistivity ln(ρ(1/T)) (a) and the Seebeck coefficient α(1/T) (b) $Lu_{1-x}Sc_xNiSb$; 1 – x=0.1; 2 – x=0.07; 3 – x=1; 4 – x=0.04; 5 – x=0; 6 – x=0.01

The change in the values of the resistivity ln(ρ(1/*T*)) $Lu_{1-x}Sc_xNiSb$ is described by the known expression (1):

$$\rho^{-1}(T) = \rho_1^{-1} \exp\left(-\frac{\varepsilon_1^{\rho}}{k_B T}\right) + \rho_3^{-1} \exp\left(-\frac{\varepsilon_3^{\rho}}{k_B T}\right), \quad (1)$$

where the first high-temperature term describes the activation of current carriers $\varepsilon_1^{\rho}(x)$ from the Fermi level ε_F to the level of continuous energy zones, and the second, low-temperature term, is the jumping conductivity at impurity states $\varepsilon_3^{\rho}(x)$ with energies close to the Fermi level ε_F.

Temperature dependences of the Seebeck coefficient α(1/*T*) $Lu_{1-x}Sc_xNiSb$ (Fig. 6*b*) are described using expression (2) [18]:

$$\alpha = \frac{k_B}{e}\left(\frac{\varepsilon_i^{\alpha}}{k_B T} - \gamma + 1\right), \quad (2)$$

where γ is a parameter that depends on the nature of the scattering mechanism. From high- and low-temperature activation regions of the α(1/*T*) dependence, the values of activation energies $\varepsilon_1^{\alpha}(x)$ and $\varepsilon_3^{\alpha}(x)$, respectively, were calculated, which, as shown in [10], are proportional to the amplitude of large-scale fluctuation of continuous energy zones and small-scale fluctuation of heavily doped and compensated semiconductors [17].

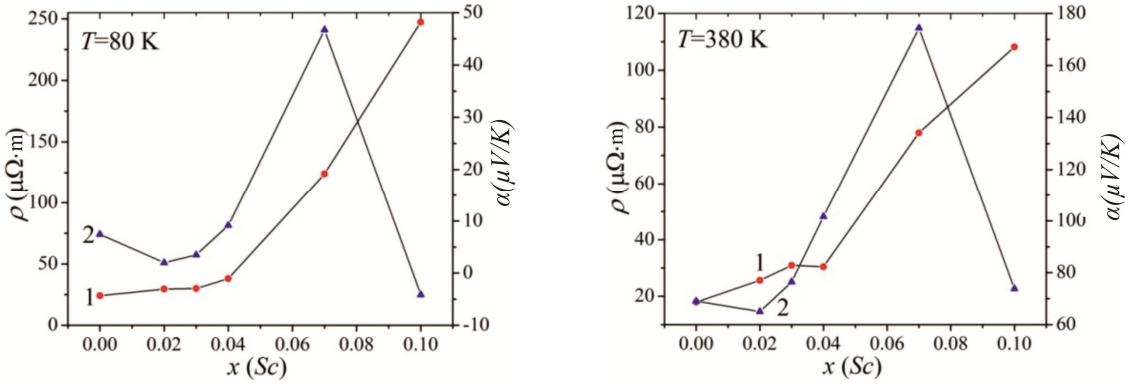

Fig. 7. Change in the values of resistivity ρ(x,T) (1) and the Seebeck coefficient α(x,T) (2) $Lu_{1-x}Sc_xNiSb$ at different temperatures

Thus, in the case of *p-LuNiSb*, the Fermi level ε_F is located at a distance $\varepsilon_1^{\rho} = 10.2$ meV from the valence band ε_V, and the amplitude of modulation of continuous energy bands is $\varepsilon_1^{\alpha} = 35.7$ meV. For the *p-ScNiSb* semiconductor, the Fermi level ε_F lies at a distance $\varepsilon_1^{\rho} = 30.1$ meV from the valence band ε_V, and the amplitude of modulation of the continuous energy bands is $\varepsilon_1^{\alpha} = 23.1$ meV. High values of activation energy ε_1^{α} in both *p-LuNiSb* and *p-ScNiSb* semiconductors indicate the presence of a significant number of uncontrolled donors, and the position of the Fermi level ε_F is determined by the ratio of concentrations of ionized acceptors and donors. And if the nature of the acceptors in *p-LuNiSb* and *p-ScNiSb* is due to the presence of structural defects in the form of vacancies, the origin of the donors lies in the plane of purity of the original components and sampling technology.

Note that only in the semiconductors *p-LuNiSb*, $Lu_{0.93}Sc_{0.07}NiSb$, $Lu_{0.90}Sc_{0.10}NiSb$ and *p-ScNiSb* in the low-temperature regions of the dependences $\ln(\rho(1/T))$ there are activation regions, indicating the mechanism of hopping ε_3^{ρ} localized states. On the other hand, the presence of ε_3^{ρ}-conductivity in a *p*-type semiconductor with a significant concentration of acceptors (vacant nature of defects in the structure of *p-LuNiSb* and *p-ScNiSb*) indicates the presence of a compensating donor impurity. And if in the form of *p-LuNiSb* and *p-ScNiSb* the presence of donors can be explained by the degree of purity of the components and the peculiarities of its synthesis and homogenizing annealing, then what generates jump ε_3^{ρ}-conductivity at concentrations *Sc*, $x = 0.07$ та $x = 0.10$?

And why for other samples of $Lu_{1-x}Sc_xNiSb$ at low temperatures the values of resistivity increase with increasing temperature (metallic conductivity)?

The answers to these questions lie in the plane of changes in the structure of $Lu_{1-x}Sc_xNiSb$, which will be shown below. Metallization of low-temperature conductivity for individual $Lu_{1-x}Sc_xNiSb$ samples indicates the close location of the Fermi level ε_F to the valence band flow level, which significantly facilitates the ionization of acceptors and the appearance of a significant number of free holes of the valence band ε_V. It is known that the activation energy of the jumping conductivity ε_3^{ρ} shows the degree of filling of holes in the *p*-type semiconductor of the conductivity of small-scale fluctuations. As soon as the holes are filled with small-scale fluctuations, the activation of the holes between the potential wells will not be carried out, and there will be no low-temperature activation sites on the resistivity dependences $\ln(\rho(1/T))$. It is obvious that in samples $Lu_{1-x}Sc_xNiSb$, $x = 0.01 – 0.04$, there is a significant number of ionized acceptors at low temperatures, which leads to overlapping of wave functions of impurity states near the Fermi level ε_F and, as a consequence, to the absence of jumping mechanism ε_3^{ρ}-conductivity. In this case, the impurity acceptor zone intersects with the valence band ε_V, forming a "tail", which is manifested by metallic conductivity at low temperatures. These experimental results are close to those calculated when modeling the distribution of DOS for the disordered variant of the $Lu_{1-x}Sc_xNiSb$ structure (Fig. 4*b*).

Fig. 8*a* shows the change in the values of the activation energy of current carriers ε_1^{ρ} from the Fermi level ε_F to the valence band flow level (positive values of the Seebeck coefficient $\alpha(x,T)$ (Figs. 6*b*, 7)). We can see that doping the base semiconductor *p-LuNiSb* with a neutral impurity *Sc* leads to a drift of the Fermi level ε_F from the flow rate of the valence band towards the middle of the band gap ε_g. Recall that in *p-LuNiSb* the Fermi level was at a distance $\varepsilon_1^{\rho} = 10.2$ meV from the valence band ε_V, and in the case of $Lu_{1-x}Sc_xNiSb$, $x = 0.10$, at a distance $\varepsilon_1^{\rho} = 67.9$ meV. This is possible either in the case of the emergence and increase in the number of donors, or a decrease in the number of acceptors with a constant number of donors.

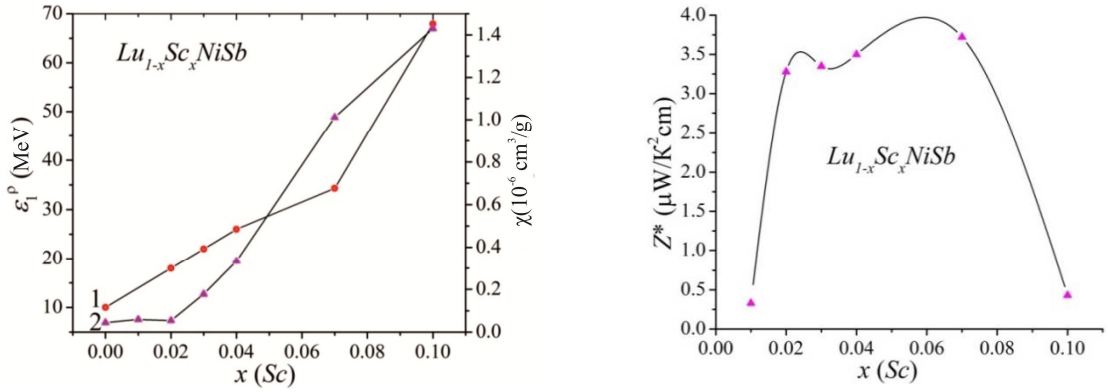

a *b*

Fig. 8. Change in the values of activation energy $\varepsilon_1^{\alpha}(x)$ (1) and specific magnetic susceptibility $\chi(x)$ (2) (a) and thermoelectric power Z (b) $Lu_{1-x}Sc_xNiSb$*

In the analysis of structural changes, we noted that as a result of the introduction of *Sc* atoms into the structure of the *LuNiSb* compound, it is possible for *Sc* atoms to occupy vacancies in position 4*a*, which simultaneously eliminates the structural defect of acceptor nature and the corresponding acceptor level. This creates a structural defect of donor nature with the appearance in the band gap ε_g of the corresponding donor band ε_D^1, which supplies free electrons, making the semiconductor $Lu_{1-x}Sc_xNiSb$ strongly doped and compensated. This mechanism of structural changes of $Lu_{1-x}Sc_xNiSb$, which generate the appearance of the donor zone ε_D^1, is the most real in the semiconductor and is consistent with the results of kinetic and energy studies.

The following interesting feature follows from the nature of the behavior of $\varepsilon_1^{\rho}(x)$ $Lu_{1-x}Sc_xNiSb$ (Fig. 8*a*). We can see that at the concentration range $x = 0 - 0.07$ the change of activation energy values $\varepsilon_1^{\rho}(x)$ is almost linear, and the velocity of the Fermi level ε_F from the valence band ε_V is constant and is $\Delta\varepsilon_F/\Delta x = 4.9$ meV/%*Sc*. At a concentration of $x \geq 0.07$, the angle of inclination of the dependence $\varepsilon_1^{\rho}(x)$ becomes steeper, which indicates an increase in the velocity of the Fermi level ε_F from the valence band ε_V to $\Delta\varepsilon_F/\Delta x = 11.2$ meV/%*Sc*. Different velocities of the Fermi level ε_F from the valence band ε_V to the middle of the band gap ε_g $Lu_{1-x}Sc_xNiSb$ show different velocities of generation of structural defects of acceptor and donor nature. It can be seen that at the concentration $x \geq 0.07$ the number of donors grows ~2 times faster than at the site $x = 0 - 0.07$. And the reason for this is different changes in the crystal structure of $Lu_{1-x}Sc_xNiSb$ depending on the concentration of *Sc* impurity atoms.

The results of changes in the values of resistivity $\rho(x,T)$, the Seebeck coefficient $\alpha(x,T)$ (Fig. 7) and Fermi level ε_F (Fig. 8*a*, curve 1) are consistent with the results of experimental measurements of magnetic $\chi(x)$ $Lu_{1-x}Sc_xNiSb$, $x = 0 - 0.10$, at room temperature (Fig. 8*a*, curve 2). Studies have shown that the $Lu_{1-x}Sc_xNiSb$ semiconductor is a Pauli paramagnet in which the magnetic susceptibility is determined exclusively by the electron gas and is proportional to the density of states at the Fermi level ε_F. As can be

seen from Fig. 8*a*, curve 2, the dependence $\chi(x)$, as well as $\rho(x,T)$ and $\alpha(x,T)$ (Fig. 7), has a plateau in the area of concentrations $x = 0 – 0.02$, which we associate with insignificant concentration of free electrons generated by the formed donor band ε_D[1]. At higher concentrations *Sc*, the rate of change of the magnetic susceptibility $\chi(x)$ $Lu_{1-x}Sc_xNiSb$, as well as $\rho(x,T)$ and $\alpha(x,T)$, increases, showing an increase in the rate of free electron generation.

Thus, the study of electrokinetic, energy and magnetic properties of $Lu_{1-x}Sc_xNiSb$ showed at different concentrations different rates of generation of structural defects of acceptor and donor nature, which is due to different mechanisms of *Sc* atoms entering the semiconductor matrix. However, this issue requires additional research, including structural, and modeling of the electronic structure of the semiconductor solid solution $Lu_{1-x}Sc_xNiSb$ under different conditions of entry into the structure of *Sc* atoms, and the above results will serve as reference points in the calculations.

Studies of the solid solution $Lu_{1-x}Sc_xNiSb$ showed that it is a promising thermoelectric material at concentrations $x = 0.02 – 0.07$ with high values of the thermoelectric power factor (Fig. 8*b*).

Conclusions

The complex nature of structural changes has been established as a result of a comprehensive study of crystal and electronic structures, thermodynamic, kinetic, energy and magnetic properties of $Lu_{1-x}Sc_xNiSb$ thermoelectric material obtained by doping *p-LuNiSb* with *Sc* atoms by substituting atoms in 4*a* crystallographic position. It is shown that, depending on the concentration of *Sc* atoms, they can occupy different crystallographic positions in the $Lu_{1-x}Sc_xNiSb$ semiconductor matrix, which leads to different rates of generation of structural defects of acceptor and donor nature. The ratio of the concentrations of existing defects of donor and acceptor nature determines the position of the Fermi level ε_F and the conduction mechanisms in $Lu_{1-x}Sc_xNiSb$. The investigated solid solution $Lu_{1-x}Sc_xNiSb$ is a promising thermoelectric material.

References

1. Karla I., Pierre J., Skolozdra R.V. (1998). Physical properties and giant magnetoresistance in *RNiSb* compounds. *J. Alloys Compd*., 265, 42–48.
2. Romaka V.V., Romaka L., Horyn A., Rogl P., Stadnyk Yu., Melnychenko N., Orlovskyy M., Krayovskyy V. (2016). Peculiarities of thermoelectric half-Heusler phase formation in *Gd-Ni-Sb* and *Lu-Ni-Sb* ternary systems. *J. Solid State Chem*., 239, 145–152.
3. Wolańska I., Synoradzki K., Ciesielski K., Załęski K., Skokowski P., Kaczorowski D. (2019). Enhanced thermoelectric power factor of half-Heusler solid solution $Sc_{1-x}Tm_xNiSb$ prepared by high-pressure high-temperature sintering method. *Materials Chemistry and Physics*, 227, 29–35.
4. Romaka V.A, Stadnyk Yu., Romaka L., Krayovskyy V., Horyn A., Klyzub P., Pashkevych V. (2020). Study of structural, electrokinetic and magnetic characteristics of the $Er_{1-x}Zr_xNiSb$ Semiconductor. *J. Phys. Chem. Sol. State*, 21(4), 689-694.
5. Romaka V.A., Stadnyk Yu.V., Romaka L.P., Pashkevych V.Z., Romaka V.V., Horyn A.M., Demchenko P.Yu. (2021). Study of structural, thermodynamic, energy, kinetic and magnetic properties of thermoelectric material $Lu_{1-x}Zr_xNiSb$. *J. Thermoelectricity*, 1, 32–50.
6. Romaka V.A, Stadnyk Yu., Romaka L., Krayovskyy V., Klyzub P., Pashkevych V., Horyn A., Garanyuk P. (2021). Synthesis and Electrical Transport Properties of $Er_{1-x}Sc_xNiSb$ Semiconducting Solid Solution. *J. Phys. Chem. Sol. State*, 22(1), 146-152.
7. Romaka V.V., Romaka L., Horyn A., Stadnyk Yu. (2021). Experimental and theoretical

investigation of the *Y–Ni–Sb* and *Tm–Ni–Sb* systems, *J. Alloys Compd.*, 855, 157334–12.

8. Anatychuk L.I. (1979). *Termoelementy i termoelectricheskiie ustroistva. Spravochnik.* [*Thermoelements and thermoelectric devices*. *Reference book*]. Kyiv: Naukova dumka [in Russian].
9. Romaka V.V., Romaka L.P., Krayovskyy V.Ya., Stadnyk Yu.V. (2015). *Stanidy ridkisnozemelnykh ta perekhidnykh metaliv* [*Stannides of rare earth and transition metals*] Lviv: Lvivska Polytechnika [in Ukrainian].
10. Romaka V.A., Stadnyk Yu.V., Krayovskyy V.Ya., Romaka L.P., Guk O.P., Romaka V.V., Mykyuchuk M.M., Horyn A.M. (2020). *Novitni termochutlyvi materialy ta peretvoriuvachi temperatury* [*New thermosensitive materials and temperature converters*]. Lviv, Lvivska Polytechnika [in Ukrainian].
11. Roisnel T., Rodriguez-Carvajal J. (2001). WinPLOTR: a windows tool for powder diffraction patterns analysis. *Mater. Sci. Forum*, Proc. EPDIC7 378–381, 118–123.
12. Babak V.P., Shchepetov V.V. (2018). Wear resistance of amorphous-crystalline coatings with lubricants. *J. Friction and Wear*, 39(1), 38–43.
13. Akai H. (1989). Fast Korringa-Kohn-Rostoker coherent potential approximation and its application to FCC *Ni-Fe* systems. *J. Phys.: Condens. Matter*., 1, 8045–8063.
14. Moruzzi V.L., Janak J.F., Williams A.R. (1978). *Calculated electronic properties of metals.* NY: Pergamon Press.
15. Savrasov S.Y. (1996). Linear-response theory and lattice dynamics: A muffin-tin-orbital approach. *Phys. Rev. B*, 54(23), 16470–16486.
16. Momma K., Izumi F. (2008). VESTA: a three-dimensional visualization system for electronic and structural analysis. *J. Appl. Crystallogr*., 41, 653–658.
17. Shklovskii B.I. and Efros A.L. (1984). *Electronic properties of doped semiconductors* NY: Springer; (1979) Moscow: Nauka.
18. Mott N.F., Davis E.A. (1979). *Electron processes in non-crystalline materials.* Oxford: Clarendon Press.

Submitted 06.04.2021

Ромака В.А., *док. тех. наук*, *професор*[1]
Стадник Ю.В., *канд. хім. наук*[2]
Ромака В.В., *док. тех. наук*,
канд. хім. наук, *професор*[3]
Демченко П.Ю., *канд. хім. наук*[2]
Ромака Л.П., *канд. хім. наук*[2]
Пашкевич В. З., *канд. техн. наук*[1]
Горинь А.М., *канд. хім. наук*[2]
Гопернюк А. Я., *канд. техн. наук*[1]

[1]Національний університет "Львівська політехніка",
вул. С. Бандери, 12, Львів, 79013, Україна;
[2]Львівський національний університет ім. І. Франка,
вул. Кирила і Мефодія, 6, Львів, 79005, Україна;
[3]Technische Universität Dresden, Bergstrasse 66,
01069 Dresden, Germany

ДОСЛІДЖЕННЯ ВЛАСТИВОСТЕЙ НОВОГО ТЕРМОЕЛЕКТРИЧНОГО МАТЕРІАЛУ $Lu_{1-x}Sc_xNiSb$

Досліджено кристалічну та електронну структури, термодинамічні, кінетичні, енергетичні та магнітні властивості термоелектричного матеріалу $Lu_{1-x}Sc_xNiSb$ за температур T=80–400 K. У залежності від концентрації легуючого компоненту у твердому розчині $Lu_{1-x}Sc_xNiSb$ встановлено різні механізмами входження атомів Sc у матрицю напівпровідника, що приводить до різних швидкостей генерування структурних дефектів акцепторної та донорної природи. Співвідношення концентрацій наявних дефектів донорної та акцепторної природи визначає у $Lu_{1-x}Sc_xNiSb$ положення рівня Фермі ε_F та механізми провідності. Досліджений твердий розчин $Lu_{1-x}Sc_xNiSb$ є перспективним термоелектричним матеріалом.
Ключові слова: електронна структура, електроопір, коефіцієнт термо-ерс. *Бібл. 18, рис. 8.*

Ромака В.А., *док. тех. наук*, *профессор*[1]
Стаднык Ю.В., *канд. хим. наук*[2]
Ромака В.В., *док. тех. наук*,
канд. хим. наук, *профессор*[3]
Демченко П.Ю., *канд. хим. наук*[2]
Ромака Л.П., *канд. хим. наук*[2]
Пашкевич В. З., *канд. техн. наук*[1]
Горынь А.М., *канд. хим. наук*[2]
Гопернюк А. Я., *канд. техн. наук*[1]

[1]Национальный университет "Львовская политехника",
ул. С. Бандеры, 12, Львов, 79013, Украина,
e-mail: vromaka@polynet.lviv.ua;
[2]Львовский национальный университет имени Ивана Франко,
ул. Кирилла и Мефодия, 6, Львов, 79005, Украина,
e-mail: lyubov.romaka@lnu.edu.ua
[3]Technische Universität Dresden, Bergstrasse 66, 01069
Dresden, Германия

ИССЛЕДОВАНИЕ СВОЙСТВ НОВОГО ТЕРМОЭЛЕКТРИЧЕСКОГО МАТЕРИАЛА $Lu_{1-x}Sc_xNiSb$

Исследованы кристаллическая и электронная структуры, термодинамические, кинетические, энергетические и магнитные свойства термоэлектрического материала. $Lu_{1-x}Sc_xNiSb$при температуре T = 80-400 K. В зависимости от концентрации легирующего компонента в твердом растворе $Lu_{1-x}Sc_xNiSb$ установлены различные механизмы вхождения атомов Sc в матрицу полупроводника, что приводит к разным скоростям генерирования структурных дефектов акцепторной и донорной природы. Соотношение концентраций имеющихся дефектов донорной и акцепторной природы определяет положение уровня Ферми ε_F и механизмы проводимости $Lu_{1-x}Sc_xNiSb$. Исследованный твердый раствор $Lu_{1-x}Sc_xNiSb$ является перспективным термоэлектрическим материалом. Библ. 18, рис. 8.
Ключевые слова: электронная структура, электросопротивление, коэффициент термоЭДС.

References

1. Karla I., Pierre J., Skolozdra R.V. (1998). Physical properties and giant magnetoresistance in *RNiSb* compounds. *J. Alloys Compd.*, 265, 42–48.
2. Romaka V.V., Romaka L., Horyn A., Rogl P., Stadnyk Yu., Melnychenko N., Orlovskyy M., Krayovskyy V. (2016). Peculiarities of thermoelectric half-Heusler phase formation in *Gd-Ni-Sb* and *Lu-Ni-Sb* ternary systems. *J. Solid State Chem.*, 239, 145–152.
3. Wolańska I., Synoradzki K., Ciesielski K., Załęski K., Skokowski P., Kaczorowski D. (2019). Enhanced thermoelectric power factor of half-Heusler solid solution $Sc_{1-x}Tm_xNiSb$ prepared by high-pressure high-temperature sintering method. *Materials Chemistry and Physics*, 227, 29–35.
4. Romaka V.A, Stadnyk Yu., Romaka L., Krayovskyy V., Horyn A., Klyzub P., Pashkevych V. (2020). Study of structural, electrokinetic and magnetic characteristics of the $Er_{1-x}Zr_xNiSb$ Semiconductor. *J. Phys. Chem. Sol. State*, 21(4), 689-694.
5. Romaka V.A., Stadnyk Yu.V., Romaka L.P., Pashkevych V.Z., Romaka V.V., Horyn A.M., Demchenko P.Yu. (2021). Study of structural, thermodynamic, energy, kinetic and magnetic properties of thermoelectric material $Lu_{1-x}Zr_xNiSb$. *J. Thermoelectricity*, 1, 32–50.
6. Romaka V.A, Stadnyk Yu., Romaka L., Krayovskyy V., Klyzub P., Pashkevych V., Horyn A., Garanyuk P. (2021). Synthesis and Electrical Transport Properties of $Er_{1-x}Sc_xNiSb$ Semiconducting Solid Solution. *J. Phys. Chem. Sol. State*, 22(1), 146-152.
7. Romaka V.V., Romaka L., Horyn A., Stadnyk Yu. (2021). Experimental and theoretical investigation of the *Y–Ni–Sb* and *Tm–Ni–Sb* systems, *J. Alloys Compd.*, 855, 157334–12.
8. Anatychuk L.I. (1979). *Termoelementy i termoelectricheskiie ustroistva. Spravochnik.* [*Thermoelements and thermoelectric devices*. *Reference book*]. Kyiv: Naukova dumka [in Russian].
9. Romaka V.V., Romaka L.P., Krayovskyy V.Ya., Stadnyk Yu.V. (2015). *Stanidy ridkisnozemelnykh ta perekhidnykh metaliv* [*Stannides of rare earth and transition metals*] Lviv: Lvivska Polytechnika [in Ukrainian].
10. Romaka V.A., Stadnyk Yu.V., Krayovskyy V.Ya., Romaka L.P., Guk O.P., Romaka V.V., Mykyuchuk M.M., Horyn A.M. (2020). *Novitni termochutlyvi materialy ta peretvoriuvachi temperatury* [*New thermosensitive materials and temperature converters*]. Lviv, Lvivska Polytechnika [in Ukrainian].
11. Roisnel T., Rodriguez-Carvajal J. (2001). WinPLOTR: a windows tool for powder diffraction patterns analysis. *Mater. Sci. Forum*, Proc. EPDIC7 378–381, 118–123.
12. Babak V.P., Shchepetov V.V. (2018). Wear resistance of amorphous-crystalline coatings with lubricants. *J. Friction and Wear*, 39(1), 38–43.
13. Akai H. (1989). Fast Korringa-Kohn-Rostoker coherent potential approximation and its application to FCC *Ni-Fe* systems. *J. Phys.: Condens. Matter.*, 1, 8045–8063.
14. Moruzzi V.L., Janak J.F., Williams A.R. (1978). *Calculated electronic properties of metals.* NY: Pergamon Press.
15. Savrasov S.Y. (1996). Linear-response theory and lattice dynamics: A muffin-tin-orbital approach. *Phys. Rev. B*, 54(23), 16470–16486.
16. Momma K., Izumi F. (2008). VESTA: a three-dimensional visualization system for electronic and structural analysis. *J. Appl. Crystallogr.*, 41, 653–658.
17. Shklovskii B.I. and Efros A.L. (1984). *Electronic properties of doped semiconductors* NY: Springer; (1979) Moscow: Nauka.
18. Mott N.F., Davis E.A. (1979). *Electron processes in non-crystalline materials.* Oxford: Clarendon Press.

Submitted 06.04.2021